

COMPASS measurement of hard exclusive π^0 muoproduction cross-section

Markéta Pešková
(on behalf of the COMPASS Collaboration)

Charles University, Faculty of Mathematics and Physics, Prague, Czech Republic

E-mail: marketa.peskova@cern.ch

Abstract. One of the goals of the COMPASS experimental program is the measurement of exclusive processes. The exclusive processes, such as Deep Virtual Compton Scattering (DVCS) or Hard Exclusive Meson Production, are important inputs for constraining the General Parton Distributions (GPDs). Exclusive π^0 production is the main source of background for DVCS process, while it provides important information on chiral-odd GPDs. The dedicated GPD program started with a one month pilot run in 2012, followed by two full years of data taking in 2016-2017, using 160 GeV/c positive and negative muon beams, a liquid hydrogen target and new detectors such as a recoil proton detector and a large-angle electromagnetic calorimeter. Our results of the exclusive π^0 production from the 2012 pilot run, recently submitted to publication, are presented. Using average of both μ^+ and μ^- data, the γ^*p cross section is extracted as a function of the squared four-momentum transfer t , and of the azimuthal angle ϕ between the scattering plane and the π^0 production plane. The average kinematics of the measurement are $\langle Q^2 \rangle = 2.0$ (GeV/c)², $\langle \nu \rangle = 12.8$ GeV, $\langle x_B \rangle = 0.093$, and $\langle -t \rangle = 0.256$ (GeV/c)². A comparison of our results with the phenomenological Goloskokov-Kroll model are shown. Prospect are given on upcoming results of the 2016/17 measurement.

1. Introduction

The General Parton Distributions (GPDs) provide a comprehensive tool for describing the 3D partonic structure of the nucleon [1, 2, 3, 4, 5]. GPDs correlate the information from Parton Distribution Functions (PDFs) and form factors, encoding the longitudinal momentum fraction and the transverse spatial position of a parton. They provide an access to the total angular momentum carried by a parton in the nucleon via the Ji's relation [2]:

$$J^f(Q^2) = \frac{1}{2} \lim_{t \rightarrow 0} \int_{-1}^1 dx x [H^f(x, \xi, t, Q^2) + E^f(x, \xi, t, Q^2)]. \quad (1)$$

For each parton flavour q , there are four parton helicity-conserving (chiral even) GPDs: $H^q(x, \xi, t, Q^2)$, $\tilde{H}^q(x, \xi, t, Q^2)$, $E^q(x, \xi, t, Q^2)$, and $\tilde{E}^q(x, \xi, t, Q^2)$. There are four corresponding parton helicity-flip (chiral-odd) GPDs: $H_T^q(x, \xi, t, Q^2)$, $\tilde{H}_T^q(x, \xi, t, Q^2)$, $E_T^q(x, \xi, t, Q^2)$, and $\tilde{E}_T^q(x, \xi, t, Q^2)$. The GPDs are expected to be universal quantities, i.e. they describe the nucleon structure independently on the specific process used to obtain them. Most commonly used processes for GPDs parametrisation are Deep Virtual Compton Scattering (DVCS) and Hard Exclusive Meson Production (HEMP). DVCS is sensitive to GPDs H^q , E^q , \tilde{H}^q , and \tilde{E}^q . At leading-twist, the vector and pseudo-scalar meson productions by longitudinally polarised virtual



photons are described by the GPDs H^q and E^q , and \tilde{H}^q and \tilde{E}^q , respectively. The contribution from transversely polarised γ^* in the exclusive π^0 production is expected to be suppressed by a factor of $1/Q$ [6], where Q is the four-momentum transfer. However, measurements of exclusive π^+ production from HERMES [7] and the exclusive π^0 production from JLab CLAS and Hall A [8, 9] have shown significant contributions, which can be explained from the GPD formalism by chiral-odd GPD coupling to a twist-3 wave function [10]. In the framework of the phenomenological model of ref. [10], pseudo-scalar meson production is described by the GPDs \tilde{H}^q , \tilde{E}^q , H_T^q and $\bar{E}_T^q = 2\tilde{H}_T^q + E_T^q$. Different partonic contents of the produced mesons give different sensitivities to the GPDs. The exclusive π^0 production is particularly sensitive to the chiral-odd GPD \bar{E}_T^q . Also the current results from exclusive π^0 production at COMPASS, presented in this paper and submitted to publication, support this finding [11].

2. COMPASS spectrometer set-up

COMPASS is a fixed-target experiment situated at the high-intensity M2 beam-line of the CERN Super Proton Synchrotron (SPS). It uses either hadron or naturally longitudinally polarised muon beams in both polarities in the energy range between 50 and 280 GeV. For the GPD program the data are collected with the 160 GeV/c muon beam with a polarisation of $\pm 80\%$ [12].

COMPASS is a two-stage magnetic spectrometer comprising a tracking system with about 350 detector planes, a ring-imaging Cherenkov detector for particle identification, electromagnetic and hadronic calorimeters and muon identification system. The GPD program started with a pilot run in 2012 and continued with the data taking in 2016-17, with about ten times larger statistics collected. The COMPASS set-up has been complemented with a 2.5 m long liquid hydrogen target inserted in a large proton recoil detector CAMERA, and a new electromagnetic calorimeter ECAL0. The 4 m long proton recoil detector consists of 2 concentric barrels with 24 scintillator slabs in each barrel, giving a time of flight (ToF) measurement between the barrels. The ECAL0 calorimeter is placed right downstream from the target and allows to extend the accessible kinematic domain for DVCS and HEMP towards higher x_B , improving the efficiency of detection of exclusive events and reducing the single-photon background from π^0 and other decays. This set-up is capable of measuring the exclusive events within the kinematic domain from $x_B \sim 0.01$ to 0.15 which is complementary to other experimental facilities.

3. Event selection

The event selection exploits the over-constrained kinematics for the measured exclusive process $\mu p \rightarrow \mu' p_{recoil} \pi^0$. The π^0 mesons are selected by their dominant two-photon decay. The selected events were required to have at least two neutral clusters in the electromagnetic calorimeters, one reconstructed vertex inside the liquid-hydrogen target with an incoming muon and an identified outgoing muon, and a recoil proton candidate in CAMERA. As the kinematics is over-constrained, for a given event, the kinematics of all recoil proton candidates are compared with the corresponding predictions that are obtained using the spectrometer information only.

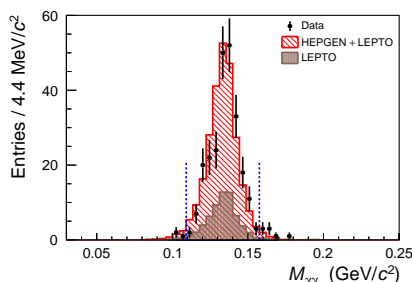


Figure 1: Invariant mass of the $\gamma\gamma$ system, and the 2.5σ cut on the π^0 mass [11].

The first left panel of fig. 2 shows the difference between the measured and the predicted value of transverse momentum Δp_T and the second panel the difference of the azimuthal angle $\Delta\phi$. Here, p_T and ϕ are given in the laboratory system. Fig. 2 (third panel) presents the difference Δz between the longitudinal position of the hit in the inner CAMERA barrel z_A and the interpolated one using the interaction vertex position and the hit position in the outer barrel z_B . Moreover the undetected mass: $M_X^2 = (k + p - k' - q' - p')^2$ is

reconstructed (see fig. 2 rightmost panel). Here, k and k' denote the four-momenta of the initial and final muon, respectively; p and p' stand for the four-momenta of target and recoiled proton, respectively; and q' the π^0 four-momentum. The applied cuts on the distributions of exclusivity variables are shown in fig. 2. Additionally, a cut on the invariant mass of the double-photon system is applied (fig. 1). Main background to exclusive π^0 muoproduction originates from the non-exclusive deep-inelastic scattering (DIS) processes. The contribution of the background is estimated by Monte Carlo simulations. LEPTO generator is used to describe the distribution of the DIS background, and HEPGEN++ for modelling the exclusive π^0 mesons. The signal and background reference samples with a wider kinematic range were used to normalise the simulations. The resulting fraction of non-exclusive (DIS) background is estimated to be $(29_{-6}^{+2})_{sys}\%$ [11].

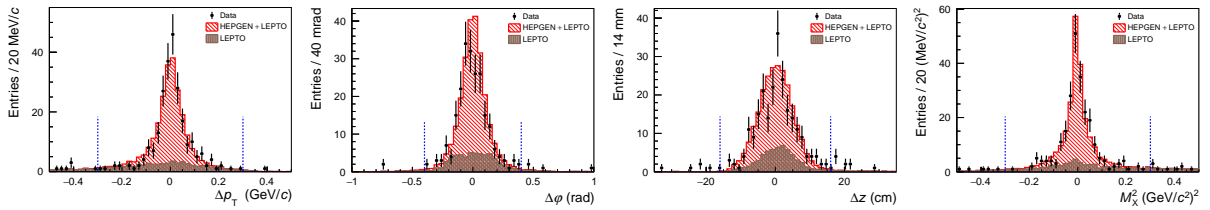


Figure 2: Distributions of the exclusivity variables: Δp_T and $\Delta\phi$ in the upper row, and Δz and the four-momentum balance in the lower row. In red is shown the sum of LEPTO and HEPGEN++ to describe the π^0 distribution and in brown the DIS distribution from LEPTO. Blue dotted vertical lines indicate the applied cuts [11, 13].

4. Results

In order to obtain the differential cross-section of the exclusive π^0 production as a function of t, ϕ, ν , and Q^2 , the collected events are corrected for the luminosity¹, the spectrometer acceptance, and a bin-wise background subtraction. The differential μp cross-section is extracted separately for μ^+ and μ^- beams. The unpolarised cross-section is obtained by averaging over the two beam polarities. The γ^*p cross section is obtained from the unpolarised muon-proton cross section by using the transverse virtual-photon flux $\Gamma = \Gamma(E_\mu, Q^2, \nu)$ [11]:

$$\frac{d^4\sigma_{\mu p}}{dQ^2 dt d\nu d\phi} = \Gamma \frac{d^2\sigma_{\gamma^* p}}{dt d\phi} \quad (2)$$

The reduced unpolarised exclusive π^0 production cross-section is formulated as follows:

$$\frac{d\sigma_{\gamma^* p}}{dt d\phi} = \frac{1}{2\pi} \left[\frac{d\sigma_T}{dt} + \epsilon \frac{d\sigma_L}{dt} \epsilon \cos(2\phi) \frac{d\sigma_{TT}}{dt} + \sqrt{2\epsilon(1+\epsilon)} \cos(\phi) \frac{d\sigma_{LT}}{dt} \right], \quad (3)$$

where $\sigma_T, \sigma_L, \sigma_{TT}$, and σ_{LT} are the structure functions; ϵ is the virtual photon polarisation parameter; and ϕ denotes the angle between the scattering and the hadronic plane. The subscript T and L represent the contribution of a transversely and longitudinally polarised γ^* , the subscripts TT and LT denote the interference terms of transversely and longitudinally polarised virtual photons of opposite helicity. The structure functions from the formula (3) are connected to convolutions of GPDs with the individual hard scattering amplitudes, for details see e.g. [11, 10]. The ϕ -dependence of the exclusive π^0 cross-section average over the measured $|t|$ -range as well as the $|t|$ -dependence after the integration over ϕ are presented in fig. 3.

¹ Integral luminosity collected with μ^+ beam: $L_{\mu^+} = 18.9 \text{ pb}^{-1}$, and with μ^- : $L_{\mu^-} = 23.5 \text{ pb}^{-1}$

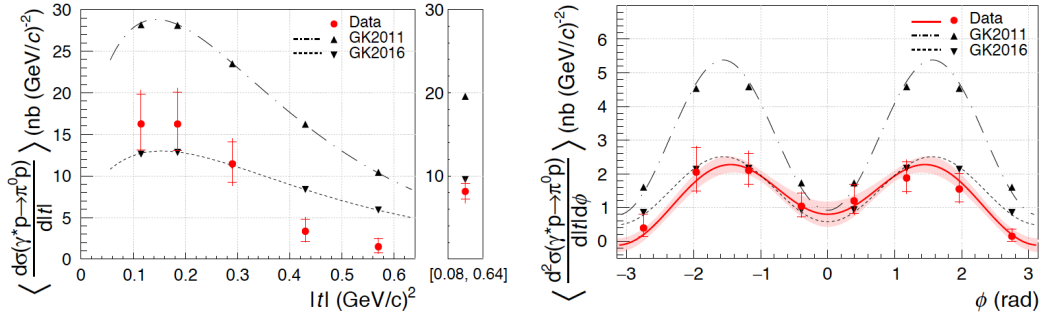


Figure 3: **Left:** The differential exclusive π^0 cross section as a function of $|t|$. **Right:** Differential exclusive π^0 cross section as a function of ϕ . Data are represented by the red dots, black dash-dotted line denotes the earlier Goloskokov-Kroll parametrisation [10], the dashed line represents the later version of the GK model adjusted to the new results in [11].

The analysis was performed on the final background-corrected data sample with average kinematics: $\langle Q^2 \rangle = 2.0$ (GeV/c) 2 , $\langle \nu \rangle = 12.8$ GeV, $\langle |t| \rangle = 0.26$ (GeV/c) 2 , and $\langle x_B \rangle = 0.093$. Our results are compared to the predictions of two versions of the Goloskokov-Kroll model, the dashed-dotted curve represents the prediction from an earlier version [10], while the dotted curve gives the later version of the model [14]. The earlier version was overshooting our result by approximately a factor two. It can be seen in fig. 3 that a difference in shape between the later model and the data still remains. The red line in fig. 3 (right panel) shows a binned maximum-likelihood fit of the ϕ -dependence of the exclusive π^0 cross section to extract the different contributions according to eq. 3:

$$\frac{d\sigma_T}{dt} + \epsilon \frac{d\sigma_L}{dt} = (8.1 \pm 0.9^{+1.1}_{-1.0}) \frac{\text{nb}}{(\text{GeV}/c)^2} \quad (4)$$

$$\frac{d\sigma_{TT}}{dt} = (-6.0 \pm 1.3^{+0.7}_{-0.7}) \frac{\text{nb}}{(\text{GeV}/c)^2} \quad (5)$$

$$\frac{d\sigma_{LT}}{dt} = (1.4 \pm 0.5^{+0.3}_{-0.2}) \frac{\text{nb}}{(\text{GeV}/c)^2} \quad (6)$$

From the results we observe a large contribution of σ_{TT} and a small positive contribution of σ_{LT} . This supports the expectation of the exclusive π^0 cross section to be dominated by transverse polarised virtual photon, which indicates a significant effect of the chiral-odd GPD \bar{E}_T . Future results from 2016-17 data-taking will still provide more statistics for constraining the Goloskokov-Kroll model.

5. References

- [1] Müller D, Robaschik D, Geyer B, Dittes F M and Hořejší J 1994 *Fortsch. Phys.* **42** 101
- [2] Ji X D 1997 *Phys. Rev. Lett.* **78** 610
- [3] Ji X D 1997 *Phys. Rev. D*, **55** 7114
- [4] Radyushkin, A V 1996 *Phys. Lett. B* **385** 333
- [5] Radyushkin, A V 1997 *Phys. Lett. D* **56** 5524
- [6] Collins J C, Frankfurt L and Strikman M 1997 *Phys. Lett. D* **56** 2982
- [7] Airapetian A *et al.* (HERMES Collaboration) 2008 *Phys. Lett. B* **659** 486
- [8] Bedlinskiy I *et al.* (CLAS collaboration) 2014 *Phys. Lett. C* **90** 025205
- [9] Defurne M *et al.* (Hall A collaboration) 2016 *Phys. Rev. Lett.* **117** 262001
- [10] Goloskokov S and Kroll P 2011 *Eur. Phys. J. A* **47** 112
- [11] Alexeev M G *et al.* 2019 (COMPASS collaboration), sub. to *Phys. Lett. B* arXiv:1903.12030
- [12] Gautheron F *et al.* (COMPASS collaboration) 2010 CERN-SPSC-2010-014, SPSC-P-340
- [13] Gorgellik M 2018 *Cross-section measurement of exclusive π^0 muoproduction and firmware design for an FPGA-based detector readout* (University of Freiburg) doi:106094/UNIFR/15945
- [14] Goloskokov S and Kroll P 2016 private communications.